LEVEL III

TECHNICAL REPORT ARBRL-TR-02134

THEORETICAL ACCURACY OF ACOUSTIC GAS TEMPERATURE MEASUREMENTS IN GUNS

Aivars Celmiņš

January 1979

US ARMY ARMAMENT RESEARCH AND DEVELOPMENT COMMAND
BALLISTIC RESEARCH LABORATORY
ABERDEEN PROVING GROUND, MARYLAND

Approved for public release; distribution unlimited.

Destroy this report when it is no longer needed.
Do not return it to the originator.

Secondary distribution of this report by originating or sponsoring activity is prohibited.

Additional copies of this report may be obtained from the National Technical Information Service, U.S. Department of Commerce, Springfield, Virginia 22161.

The findings in this report are not to be construed as an official Department of the Army position, unless so designated by other authorized documents.

The use of trade names or manufacturers' names in this report does not constitute indorsement of any commercial product.

UNCLASSIFIED
SECURITY CLASSIFICATION OF THIS PAGE (When Data Entered)

REPORT DOCUMENTATION PAGE	READ INSTRUCTIONS BEFORE COMPLETING FORM
1. REPORT NUMBER: TECHNICAL REPORT ARBRL-TR-02134	2. GOVT ACCESSION NO. / 3. RECIPIENT'S CATALOG NUMBER
4. TITLE (and Subtitle): THEORETICAL ACCURACY OF ACOUSTIC GAS TEMPERATURE MEASUREMENTS IN GUNS	5. TYPE OF REPORT & PERIOD COVERED
	6. PERFORMING ORG. REPORT NUMBER
7. AUTHOR(s): Aivars Celmiņš	8. CONTRACT OR GRANT NUMBER(s)
9. PERFORMING ORGANIZATION NAME AND ADDRESS: US Army Ballistic Research Laboratory, ATTN: DRDAR-BLB, Aberdeen Proving Ground, MD 21005	10. PROGRAM ELEMENT, PROJECT, TASK AREA & WORK UNIT NUMBERS: RDTE Project No. 1L161102AH43
11. CONTROLLING OFFICE NAME AND ADDRESS: US Army Armament Research & Development Command, Ballistic Research Laboratory (ATTN: DRDAR-BLB), Aberdeen Proving Ground, MD 21005	12. REPORT DATE: JANUARY 1979
	13. NUMBER OF PAGES: 37
14. MONITORING AGENCY NAME & ADDRESS (if different from Controlling Office)	15. SECURITY CLASS. (of this report): Unclassified
	15a. DECLASSIFICATION/DOWNGRADING SCHEDULE

16. DISTRIBUTION STATEMENT (of this Report)

Approved for public release; distribution unlimited.

17. DISTRIBUTION STATEMENT (of the abstract entered in Block 20, if different from Report)

DDC RECEIVED MAY 11 1979 B

18. SUPPLEMENTARY NOTES

19. KEY WORDS (Continue on reverse side if necessary and identify by block number)

Interior ballistics
Muzzle blast
Propellant gas temperature
Rarefaction wave velocity

20. ABSTRACT (Continue on reverse side if necessary and identify by block number) (fek)

The ejection of a projectile from a gun is followed by a flow of high pressure gases through the muzzle of the weapon. The temperature in the gas immediately after the projectile has cleared the muzzle can be measured by a recently developed acoustic temperature measurement technique. This report is a theoretical analysis of the accuracy of the new measurement technique. It is estimated that the standard errors of the temperature observations are typically about 15%. It is also shown that the technique measures an average temperature

DD FORM 1 JAN 73 1473 EDITION OF 1 NOV 65 IS OBSOLETE

313112

UNCLASSIFIED
SECURITY CLASSIFICATION OF THIS PAGE (When Data Entered)

for the first few milliseconds, instead of measuring the instantaneous initial temperature. Consequently, by this technique one cannot detect temperature excursions of less than one millisecond duration, such as predicted by one-dimensional interior ballistics theories.

TABLE OF CONTENTS

LIST OF FIGURES

1. INTRODUCTION.

A projectile is subjected during the first few milliseconds of free flight to a high pressure jet flow from the muzzle. Assessment of the projectile's behavior in this environment requires an accurate description of the jet which is typically provided by theoretical calculations. Their accuracy depends among other things on the accuracy of the assumed boundary conditions, i.e., of the conditions in the flow through the muzzle of the weapon. Therefore, one is interested to assess the accuracy of theoretically predicted muzzle flows. Such detailed predictions are routinely provided by mathematical models of the interior ballistics. Experimental determination of the flow is, on the other hand, technically difficult and is usually limited to a measurement of the projectile's velocity and to pressure measurements in the gun tube near the muzzle. The measurements do not determine the gas flow completely. Thus, different computer models of interior ballistics may predict muzzle velocities and pressures which are in agreement with observations, but postulate at the same time significantly different temperatures and densities. Independent measurement of temperatures and densities in muzzle flows are therefore of great interest theoretically as well as for practical reasons.

In a recent BRL Report [1] E. M. Schmidt, et al, have described a new temperature measuring technique which is designed to measure the initial temperature in the gas efflux. The technique is based on a measurement of sound speed in the gas and a subsequent calculation of the temperature from the sound speed. We shall give in Section 2 of this report a short description of the technique.

Measurements of temperature constitute a new data source (in addition to pressure measurements) for the validation of interior ballistics calculations. In order to use the observations for this purpose, one has to know their accuracies. In this report, we shall investigate the intrinsic accuracy of the temperature measurement technique. The particular goal of the investigation is to find quantitative limits within

[1] E. M. Schmidt, E. F. Gion and D. D. Shear, "Acoustic Thermometric Measurements of Propellant Gas Temperatures in Guns", BRL Report No. 1919, August 1976. (AD #A030359)

which the temperature measurements should agree with temperatures predicted by interior ballistics calculations of the same event.

The accuracies of the temperature measurements are affected by three sources of errors.

First, one has a limited observational accuracy which produces a computed sound speed with an error margin. This error propagates through subsequent calculations and produces a corresponding error margin for the temperature. An investigation of this error is done in Section 3, and it is based on variance propagation formulas.

Second the measurement technique possesses an intrinsic averaging property due to the finite size of the measurement apparatus. A consequence of this property is that the recorded temperature is not the instantaneous initial temperature in the gas efflux, but an average temperature for the first few milliseconds of the flow. Therefore, short duration temperature excursions (predicted by some mathematical models of interior ballistics) might not be detectable by the apparatus. A quantitative investigation of the averaging property of the technique is done in Sections 4 and 5. In Section 4 we describe typical theoretically calculated interior ballistics flows, and in Section 5 we simulate and analyze the response of the measurement apparatus to the calculated flows.

A third source of error is the approximate nature of the equation of state which provides the relation between sound speed and temperature. An investigation of this systematic error source requires an analysis of the physical properties of the combustion products, and it will not be pursued here. We notice, however, that for a comparison of temperature measurements of a real firing with interior ballistics calculations this error source is not important, because it affects measurements and calculations in the same way. The calculations depend, on the other hand, also on many other assumptions about the properties of the gas flow and propellant. Therefore, if discrepancies between measurements and calculations exist and are larger than can be caused by the first two error sources, then one can conclude that the mathematical model of the flow is inadequate. In an analysis of the response of the apparatus to theoretical flows, errors from the third source are not existent, because for theoretical flows the equation of state is given by definition.

In Section 6 of the report we summarize the conclusions which can be drawn from the simulated response of the apparatus and give quantitative limits for application of the measurement technique.

2. THE ACOUSTIC TEMPERATURE MEASUREMENT TECHNIQUE.

Technical details of the acoustic temperature measurement technique and some typical results are given in Reference 1. In this report we shall present only a short outline of the method.

The apparatus is designed to measure the sound speed c[m/s] in the gas behind the projectile. Assuming that the gas is adequately described by an ideal gas equation one can compute the gas temperature T[K] from the sound speed by

$$T = c^2 M/(\gamma R) = c^2 T_{flame}/(gf), \tag{1}$$

where M[kg/mol] is the molar mass of the gas, γ is the ratio of its specific heats, $R = 8.3143[J\ K^{-1}\ mol^{-1}]$ is the universal gas constant, $T_{flame}[K]$ is the isochoric flame temperature of the propellant which drives the projectile, $g = 9.80655[m/s^2]$ is the standard acceleration, and f[m] is the explosive "force" of the propellant.

The sound speed c is obtained by subtracting from the projectile's muzzle velocity u_M the velocity u_r of the rarefaction wave, which travels upstream into the barrel after the projectile has cleared the muzzle, i.e., by

$$c = u_M - u_r . \tag{2}$$

The setup of the apparatus for the measurement of u_M and u_r is shown schematically in Figure 1. The muzzle velocity u_M is obtained from X-rays of the projectile outside the weapon. The velocity u_r of the rarefaction wave is determined from pressure traces which are produced by two or more pressure gages in the barrel.

Let $\Delta x = x_B - x_A$ be the distance between the first and the last pressure gage (Figure 1). Then the sound speed c can be computed by

$$c = u_M - \frac{\Delta x}{t_B - t_A}, \tag{3}$$

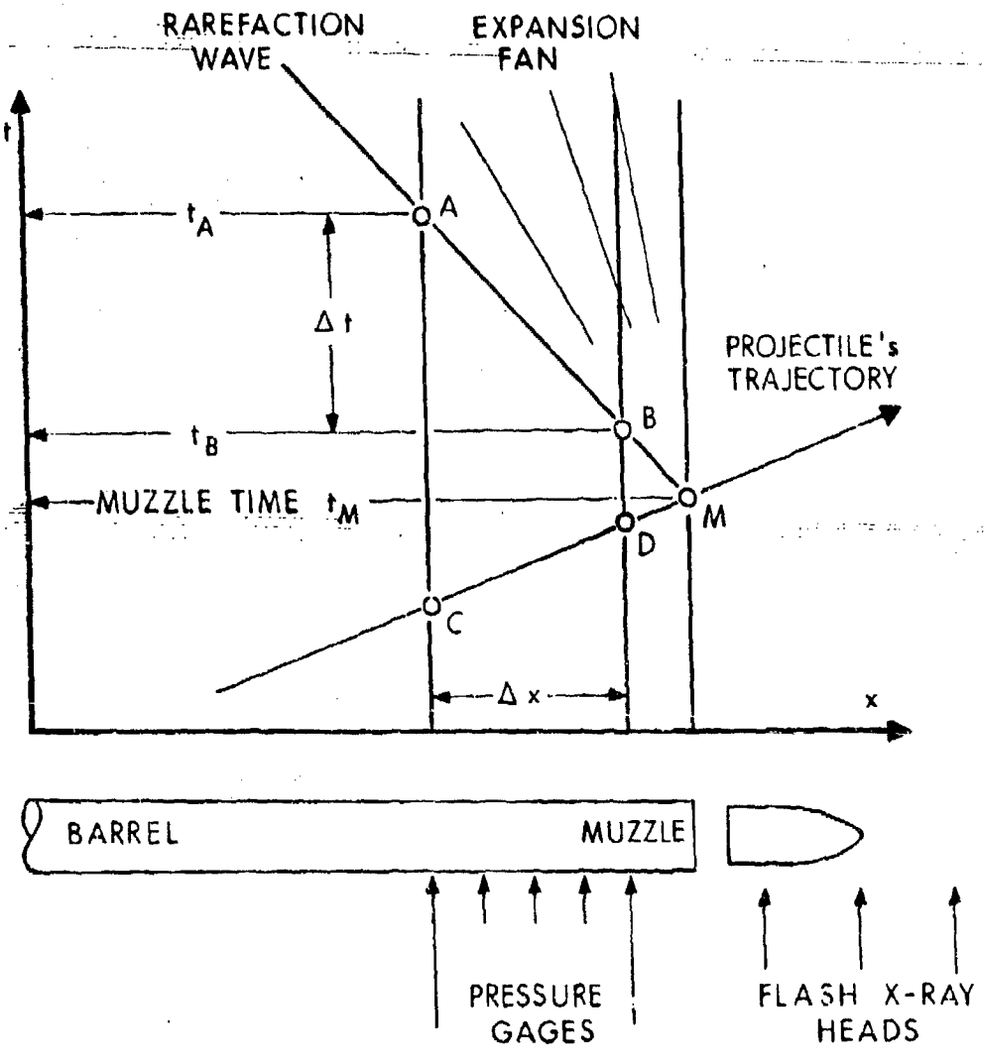

Figure 1. Schematic of the Acoustic Temperature Measurement Technique.

if one assumes that the characteristic ABM in Figure 1 is straight and the particle velocity is equal to u_M throughout the muzzle region.

Typical pressure histories at the gages are shown in Fig. 2. They were computed using a mathematical model [2,3] of the interior ballistics and they agree qualitatively with pressure traces actually observed and reproduced in Reference 1. The arrival of the rarefaction wave corresponds to a gradient discontinuity in the pressure traces and the arrival times can be determined by visual inspection of photographs of the traces.

The simple formula (3) for the sound speed is exact if all flow properties within the area ABMDC of Figure 1 are uniform. Making other assumptions about the flow, one can derive other formulas for the sound speed. Thus, assuming in ABMDC isentropy and adiabatic expansion, but permitting the pressure to be variable, the following corrected formula is derived in Reference 1:

$$c_D = \left(u_M - \frac{\Delta x}{t_B - t_A}\right)\left\{1 + \frac{3-\gamma}{\gamma-1}\left[1 - \frac{1}{\Delta t}\int_{t_B}^{t_A}\left(\frac{p}{p_D}\right)^{\frac{\gamma-1}{2\gamma}} dt\right]\right\}^{-1} \qquad (4)$$

In eq. (4), c_D and p_D are the sound speed and pressure, respectively, at node D of Figure 1, and $\Delta t = t_A - t_B$. The integral in eq. (4) is a line integral along the path BA of the rarefaction wave. If the pressure $p \equiv p_D$ along the path, then eq. (4) reduces to eq. (3). One can see from Figure 2 that generally $p/p_D < 1$ along the integration path and, therefore, c_D computed with eq. (4) is smaller than the sound speed computed with eq. (3). The integral in eq. (4) can be evaluated numerically using pressures which are provided by pressure gages between the extreme gages. The apparatus described in Reference 1 had three gages, located at 25mm, 50mm and 75mm from the muzzle of a 20mm cannon. This number of gages is sufficient for the numerical quadrature because the pressure varies smoothly along the integration path and, in addition, the pressure exponent $(\gamma - 1)/2\gamma$ is very small (typically about 0.1).

---

[2] A. K. R. Celmins, "Theoretical Basis of the Recoilless Rifle Interior Ballistics Code RECRIF", BRL Report No. 1931, September 1976. (AD #B013852L)

[3] A. K. R. Celmins, "RECRIF Users' Manual", BRL Memorandum Report 2692, October 1976.

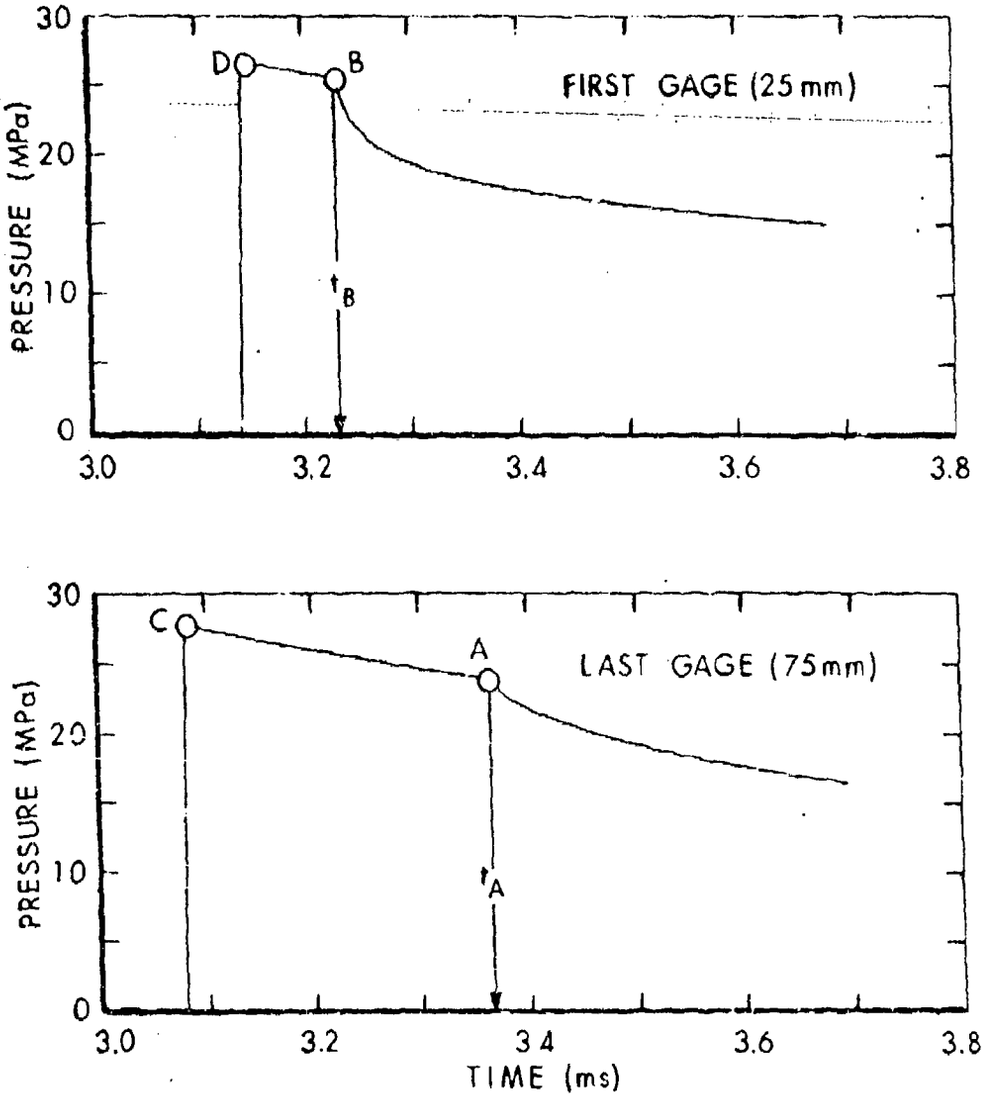

Figure 2. Pressure Histories at the Extreme Gages. Muzzle Velocity 820 m/s.

3. STANDARD OBSERVATIONAL ERRORS.

The principal idea of the acoustic temperature measurement technique is to measure the sound speed c and to compute the corresponding temperature T by eq. (1). Because T is proportional to c^2, the relative standard error of T is twice the relative standard error of c:

$$e_T/T = 2\, e_c/c. \tag{5}$$

Eq. (5) provides an estimate of e_T from estimates of e_c.

The standard error e_c of the sound speed depends on the observational errors as well as on the formula which is used to compute c. The simple formula (3) has a smaller standard error than eq. (4) because it depends on lesser measurements. The difference between the accuracies of both equations is small, however, because the additional observations (pressure) enter eq. (4) with a very small exponent. We shall, therefore, restrict our analysis to eq. (3).

For the purpose of error analysis one can consider the following quantities as directly and independently observable: the muzzle velocity u_M, the arrival times of the rarefaction wave, t_A and t_B, and the distance Δx between the pressure gages. The law of error propagation, (Reference 4) applied to eq. (3), then furnishes a formula for the standard error of the sound speed in terms of the standard errors e_{uM}, e_t and $e_{\Delta x}$ of the observables. The formula is

$$e_c = \left\{\left(\frac{\Delta x}{\Delta t}\right)^2\left[\left(\frac{e_{\Delta x}}{\Delta x}\right)^2 + 2\left(\frac{e_t}{\Delta t}\right)^2\right] + e_{uM}^2\right\}^{1/2}, \tag{6}$$

where $\Delta t = t_A - t_B$. The relative standard error of the sound speed is

$$\frac{e_c}{c} = \left\{\left(1 - \frac{u_M}{c}\right)^2\left[\left(\frac{e_{\Delta x}}{\Delta x}\right)^2 + 2\left(\frac{e_t}{\Delta t}\right)^2\right] + \left(\frac{u_M}{c}\right)^2\left(\frac{e_{uM}}{u_M}\right)^2\right\}^{1/2}. \tag{7}$$

In order to get an idea about the relative importance of the various terms in eq. (7), we substitute typical values into the equation. The ratio u_M/c is the Mach number of the flow. In the examples in this report it varies between 0.2 and 0.8.

---

[4] W. E. Demming, Statistical Adjustment of Data, J. Wiley & Sons, New York, NY, 1944.

In practical applications the Mach number will be limited probably to values below 0.6 because for larger values the rarefaction wave is difficult to detect from the pressure traces. As a convenient typical average one might assume $u_M/c = 0.5$. The values of $e_{\Delta x}/\Delta x$ and e_{uM}/u_M we assume to be of the order 0.01. With these assumptio s eq. (7) simplifies to

$$\frac{e_c}{c} \approx 0.7 \left\{ \left(\frac{e_t}{\Delta t} \right)^2 + 10^{-4} \right\}^{1/2} . \qquad (8)$$

The standard error e_t of the time readings increases with the muzzle velocity because the rarefaction wave is less pronounced in pressure traces for higher velocities. The deterioration of time readings is compensated to some extent by an increase of Δt with increasing u_M. For a Mach number ≈ 0.3 one finds from Figure 7 of Reference 1 that $\Delta t \approx 0.1$ ms and $e_t/\Delta t \approx 0.1$ or larger. This shows that in eq. (7) or (8) the time reading inaccuracies dominate over all other terms. The relative standard error of the sound speed is with these assumptions about 7%. The corresponding relative standard error of the temperature is about 14%. This value agrees in the order of magnitude with the scatter of about 10% of observed temperatures shown in Figure 12 of Reference 1. Our analysis shows that a scatter of this magnitude can be explained by inaccuracies of time readings. It is also evident that, in order to improve the overall accuracy of the technique, one has to improve in the first place the accuracies of the rarefaction wave's arrival time measurements.

The above consideration is restricted to random observational errors. In addition to these, one has systematic errors, intrinsic to the technique. We shall analyze some of the systematic errors in the next sections.

4. THEORETICAL TEST CASES.

Reference 1 describes tests of the acoustic temperature measurement technique on a 20mm cannon. The tests were carried out for muzzle velocities between 265 m/s and 910 m/s. The variation of the muzzle velocity was achieved by a variation of the amount of propellant which was used for the firing of the weapon.

In this report we chose an identical arrangement for the generation of theoretical test cases. The interior ballistics were computed using the computer code RECRIF [2,3]. The code was slightly modified for the present purposes to allow an explicit tracing of the rarefaction wave and to permit a better definition of the flow within the expansion fan region. The input parameters for the calculations are listed in Table I.

TABLE I

Input for Interior Ballistics Calculations

Weapon

Bore diameter	20mm
Barrel length	1.5m
Chamber volume	$42 \cdot 10^{-6} m^3$

Projectile

Mass	100 g
Release pressure	5 MPa

Propellant

Density	$1600\ kg/m^3$
Ratio of specific heats γ	1.25
Flame temperature	2600 K
Explosive "force"	100 kJ/kg
Combustion law exponent	0.85
Combustion law coefficient	$10^{-8} m \cdot s^{-1} \cdot Pa^{-0.85}$

Geometry: spheres with 1.0 mm diameter

Equation of state: Ideal gas with constant γ

Mass: 3g - 47.5g (several cases were computed)

Pressure gages

Six gages at 12.5mm intervals from the muzzle. For simulated temperature measurements a "First gage" was assumed at 25mm and a "Last gage" at the 75mm location. For adjustment calculations all six gages were used.

By specifying different amounts of propellant, muzzle velocities between 200 m/s and 1200 m/s were obtained. The relation between propellant mass and muzzle velocity is shown in Figure 3 which also shows experimentally observed velocities. Because the purpose of the calculations was to generate representative theoretical interior ballistic flows (and not to model a specific weapon), the agreement between experimental and calculated velocities is sufficiently close. Since calculated and observed pressures also agreed approximately, the calculated flows can be considered as adequate examples of typical theoretically computed flows in a 20mm cannon.

In the next section we shall describe the simulated response of the acoustic temperature measurement apparatus to the theoretically computed flows. To simulate this response, one has to extract from the calculations the arrival times of the rarefaction wave at gage locations, list the pressure histories at the same locations, and use these data in the temperature formulas. Because the interior ballistics calculations included an explicit tracing of the rarefaction wave front, the arrival times were obtained with high accuracy. This eliminated the major source of observational errors. A second source of error, the inaccuracy of the equation of state, is not present in a simulated response to a theoretical flow, because the equation of state is given by definition. Consequently, any differences between the gas temperatures from interior ballistics calculations and from the simulated response of the acoustic measurement technique are caused by averaging effects of the technique.

The averaging effects are small if the gas temperature varies only little within the region ABMDC of Figure 1. The variations cannot be assumed small in all cases, however. A one-dimensional treatment of interior ballistics produces necessarily a temperature peak at the basis of the projectile [5,6]. The theoretical background of the phenomenon is discussed in Reference 2, pp. 101-102, and a typical example of theoretically predicted temperature variations within the gun is shown in Figure 4. The temperature variations within the region ABMDC of observations can be quite large for high muzzle velocities. This is illustrated by Figures 5 and 6, showing theoretical temperature histories at the locations of the extreme gages in a low velocity and a moderate velocity case, respectively. In the low velocity case, Figure 5, the

[5] S. Shelton, A. Bergler and P. Saha, "Study of Heat Transfer and Erosion Rate in Gun Barrels", Air Force Armament Laboratory Technical Report TR-75-69, March 1973.

[6] R. Helser, "Hodographenverfahren für Instationäre Eindimensionale Gasströmungen", Phd Thesis, Technical University Aachen, FRG, December 1975.

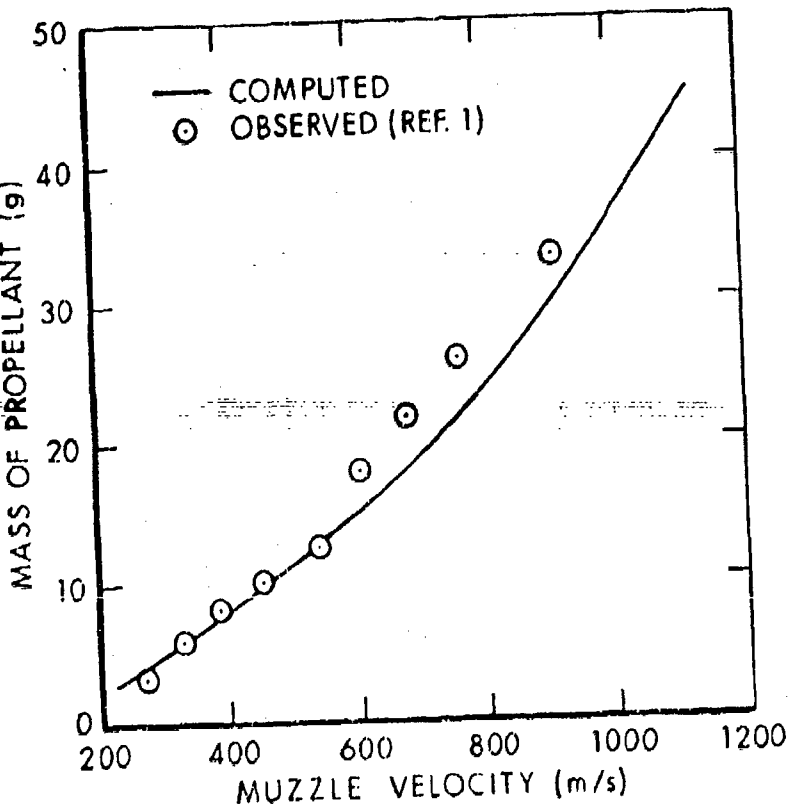

Figure 3. Computed and Observed Muzzle Velocities.

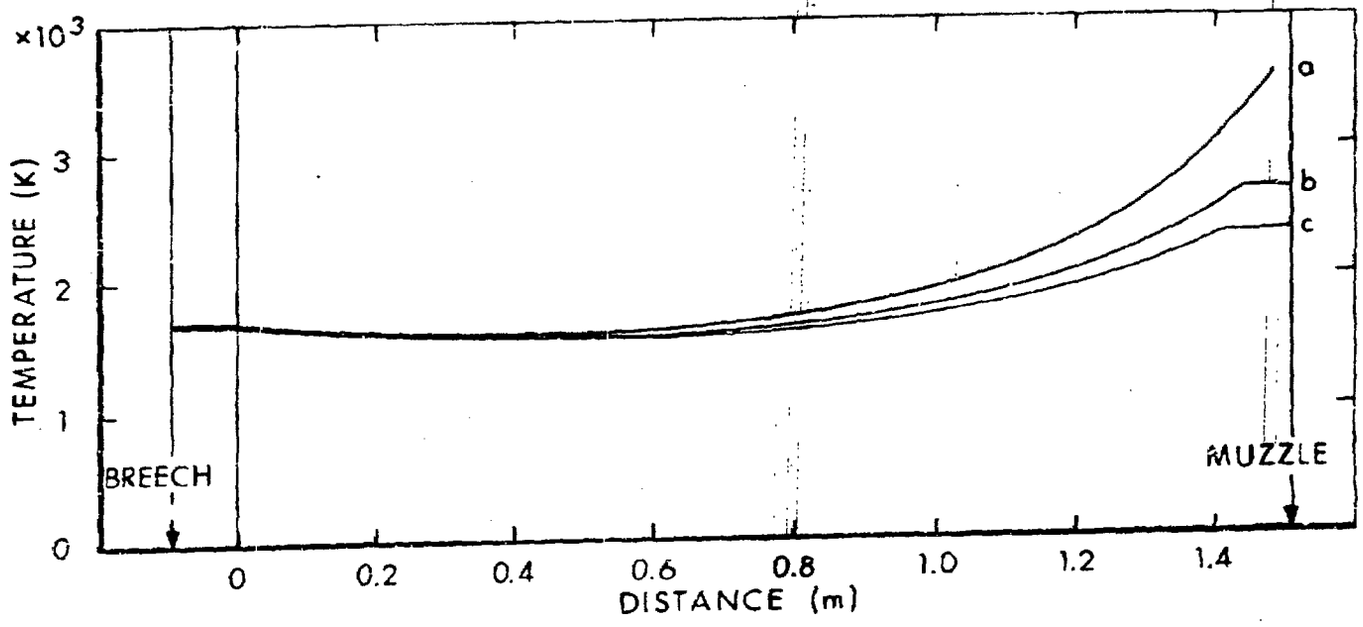

Figure 4. Temperature Profiles. Muzzle Velocity 820 m/s. The gas temperature is shown for the following times: a — 0.02 ms before muzzle time, b — 0.13 ms after muzzle time, c — 0.23 ms after muzzle time.

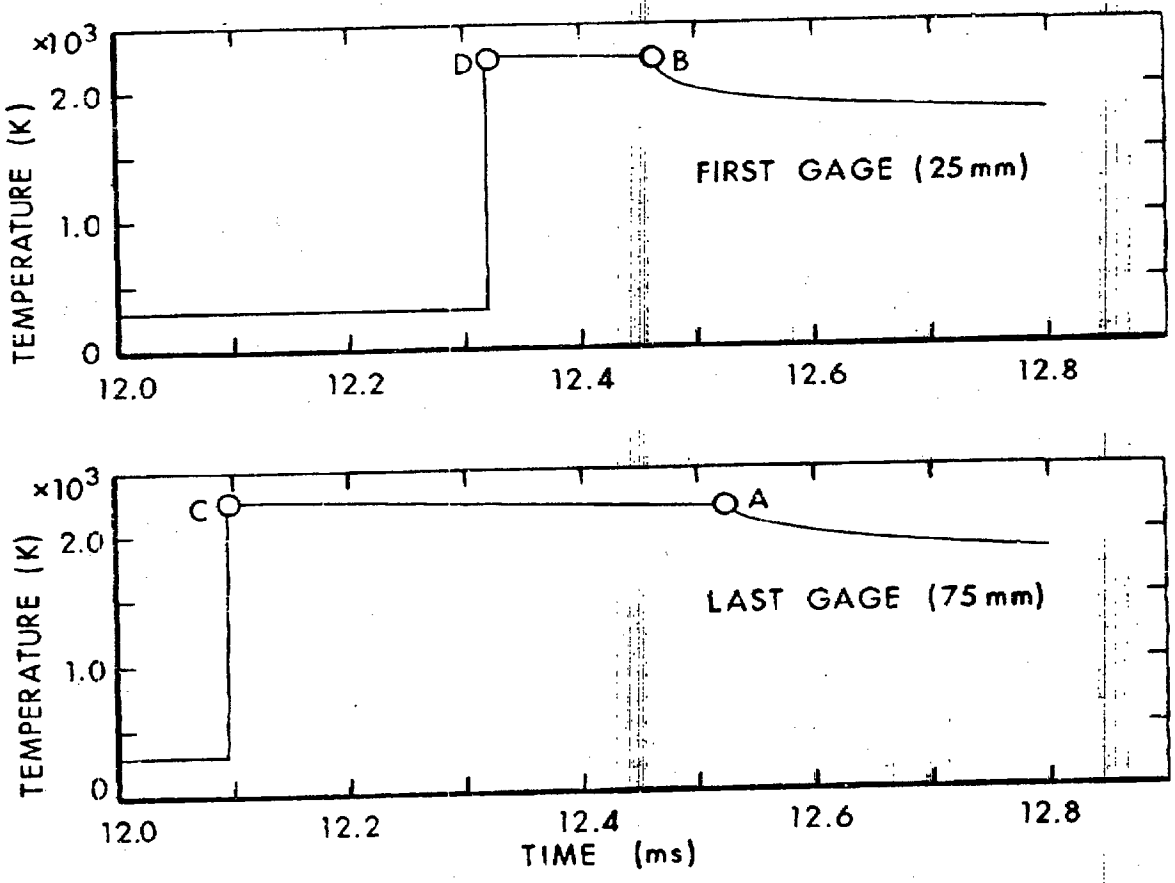

Figure 5. Temperature Histories at the Extreme Gages. Muzzle Velocity 225 m/s.

temperature difference between the nodes C and A is 60K or 3%, i.e., well below the standard observational error. In the case shown in Figure 6 the difference is about 1000K or 30% of the initial muzzle flow temperature. One can expect a strong averaging effect by the acoustic measurement technique in this case.

The temperature measurement technique breaks down at about 900 m/s for the weapon type considered here. This limit is reported in Reference 1 and it is caused by difficulties to detect the rarefaction wave in pressure traces from high velocity firings. Figure 7 shows a theoretical example of such a pressure trace. The gradient discontinuity at the node B in Figure 7 is barely visible. The reduction of the discontinuity is caused by changes of the characteristics' slope with increasing flow velocity. Figure 8 shows characteristic curves in a case with moderate muzzle velocity and Figure 9 shows corresponding curves for a high muzzle velocity. As the Mach number of the flow approaches one, the angles of intersection between the rarefaction wave (a (u-c) characteristic) and the gage lines x = const. become more acute. Consequently, the corresponding gradient discontinuities in the pressure traces become less pronounced. A theoretical limit of the method is given by a still higher muzzle velocity at which the rarefaction wave is swept out through the muzzle before it reaches the pressure gages. In the present example this occurs for a muzzle velocity of about 1160 m/s.

We reiterate that the described flow properties are based on one-dimensional mathematical modeling of the flow. Experimental verifications of the details do not exist and one application of the acoustic temperature measurements could be to provide such a verification or a rejection of the theory.

5. SIMULATED RESPONSE OF THE APPARATUS TO THEORETICAL MUZZLE FLOWS.

The response of an acoustic temperature measurement apparatus to theoretically computed muzzle flows can be simulated as follows. First, one obtains from the computed flow accurate "readings" of the arrival times of the rarefaction wave at the pressure gage locations. The time readings are substituted in eq. (3) to compute the sound speed, and the temperature is computed using eq. (1). The corrected sound speed which is given by eq. (4) can be computed using pressures along the integration path. In the present examples, the integral in eq. (4) was calculated by a trapezoidal formula using pressure readings at six pressure gage locations at 12.5mm intervals.

The results of the calculations are shown in Figure 10. The extreme curves in the figure are those of the temperatures T_D and T_A at the nodes D and A of Figure 1, respectively. The temperature at the muzzle node M is practically equal to T_D. The difference between T_D and T_A

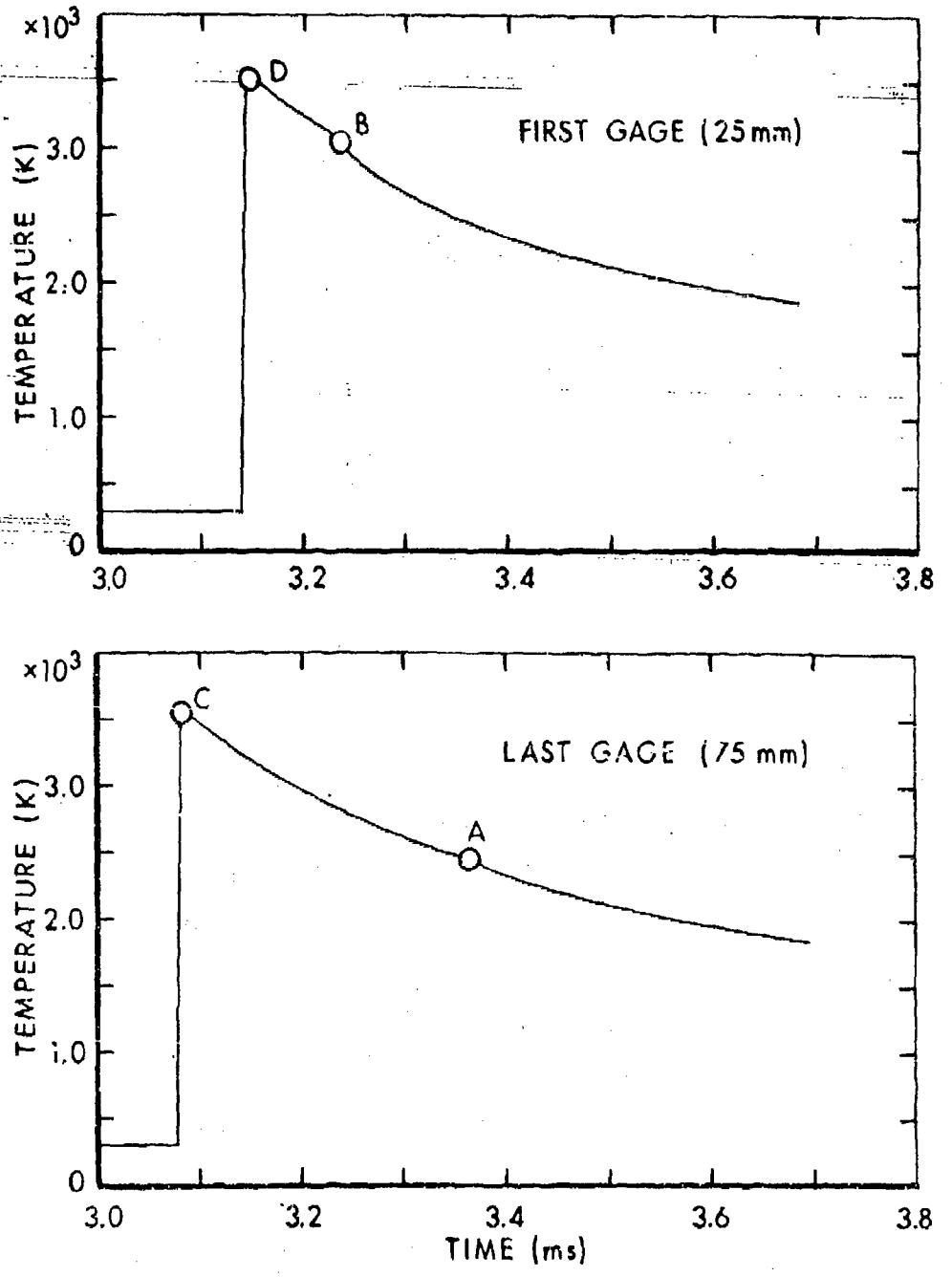

Figure 6. Temperature Histories at the Extreme Gages. Muzzle Velocity 820 m/s.

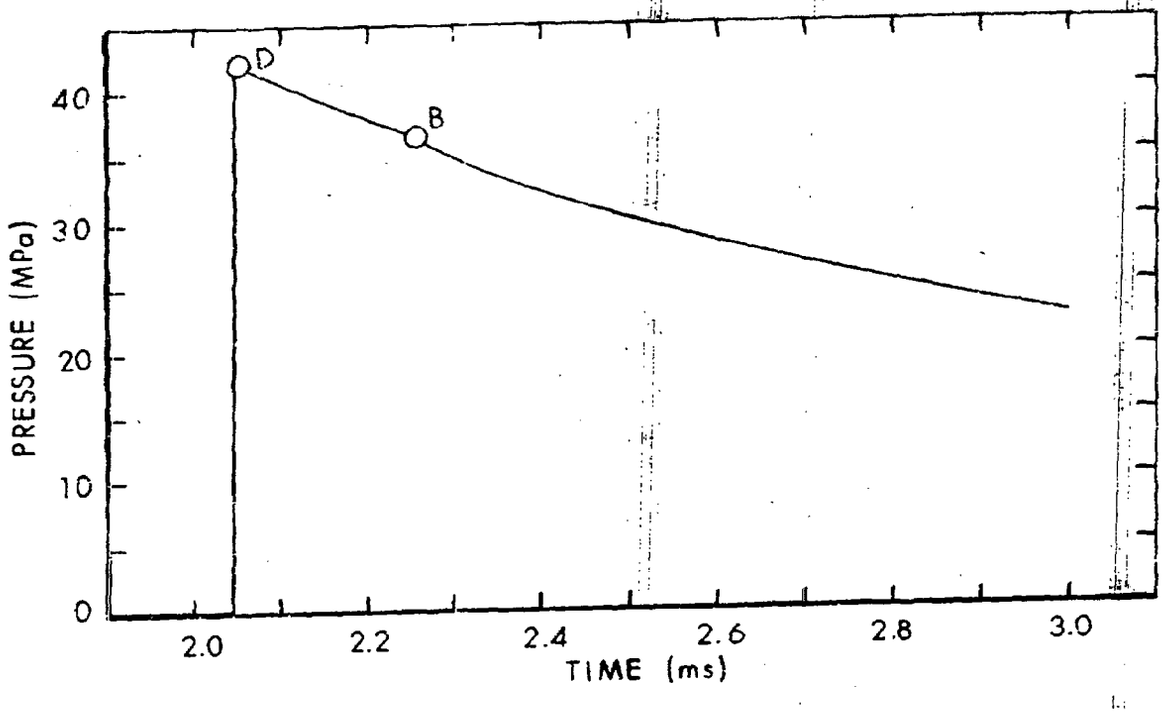

Figure 7. Pressure History at the First Gage (25mm). Muzzle Velocity 1130 m/s.

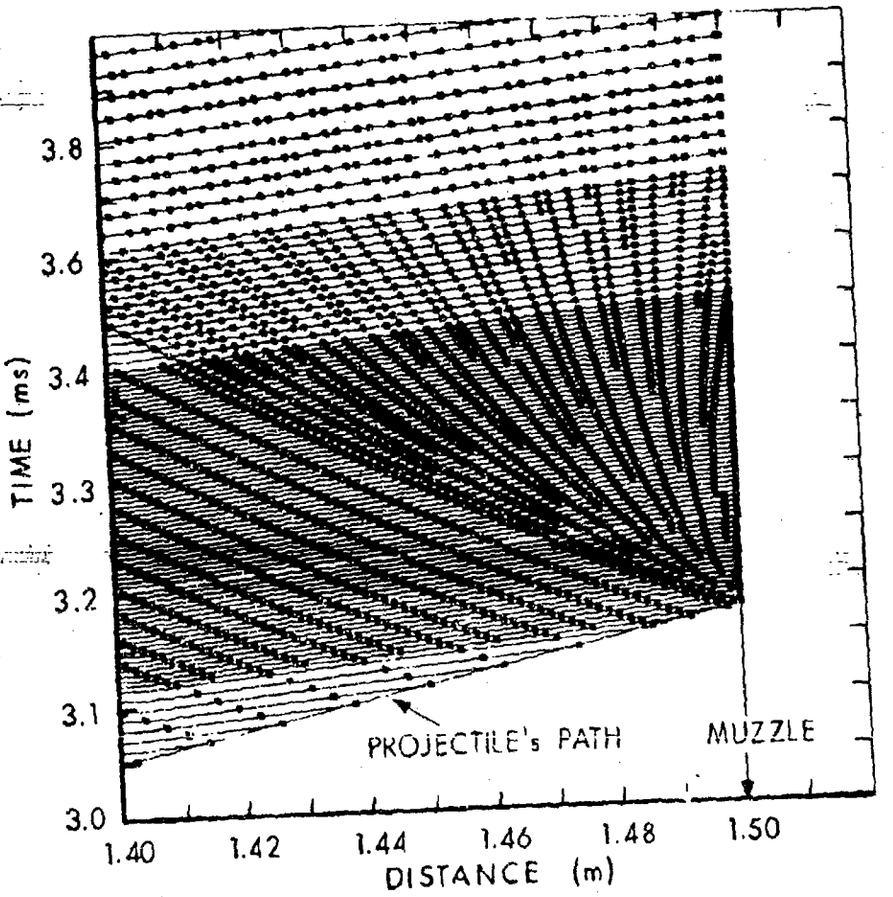

Figure 8. Computed Nodes and Characteristics in the Muzzle Region. Muzzle velocity 820 m/s. The (u+c)-characteristics and the rarefaction wave front are traced by continuous lines. The (u-c)-characteristics follow the arrangement of the nodes.

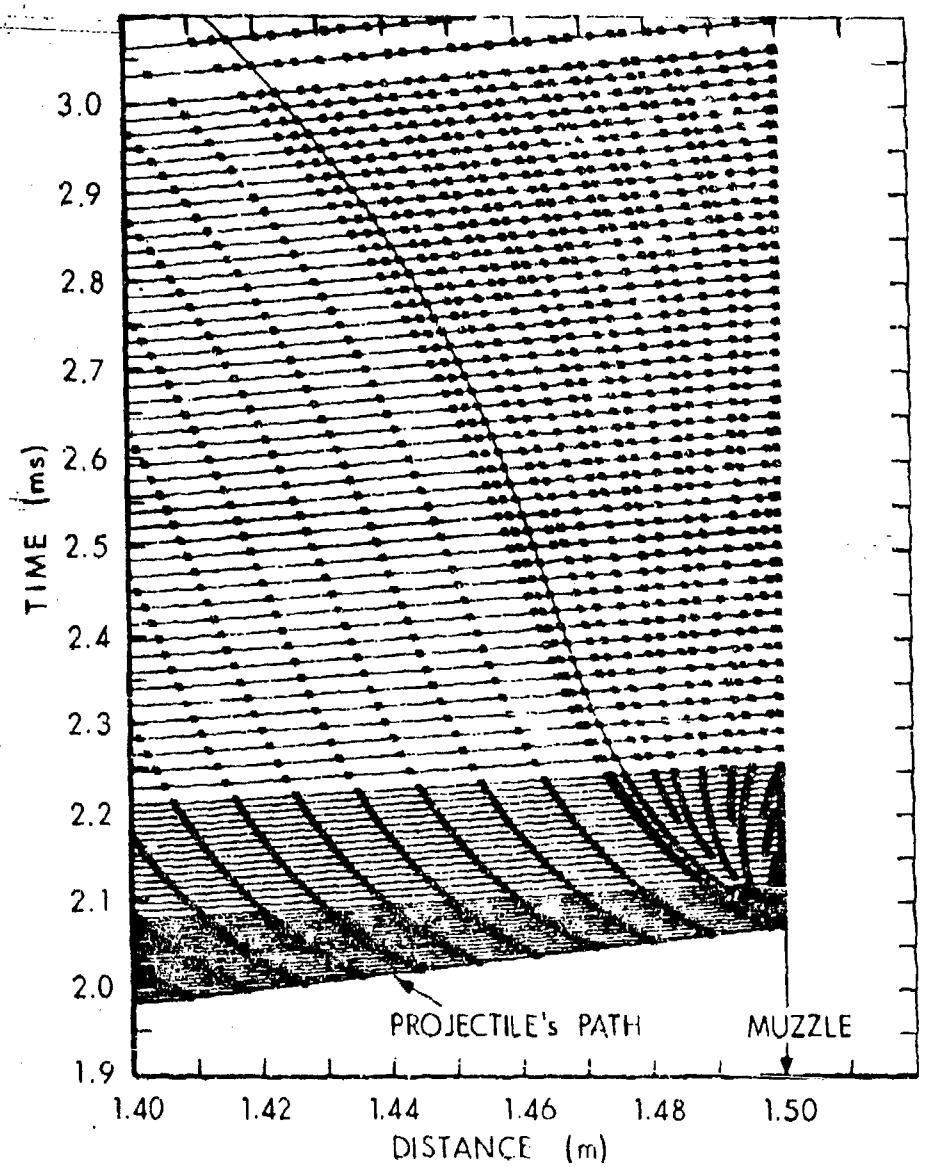

Figure 9. Computed Nodes and Characteristics in the Muzzle Region. Muzzle Velocity 1130 m/s.

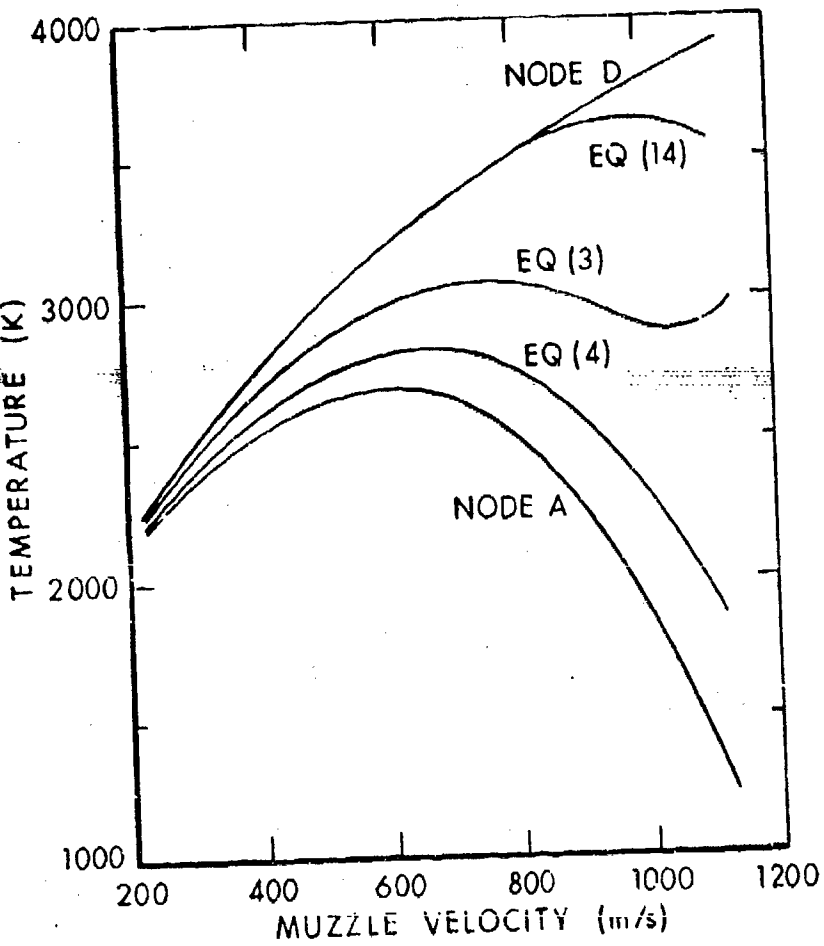

Figure 10. Gas Temperatures in the Muzzle Region.

is quite remarkable in cases with high muzzle velocity. For muzzle velocities over 600 m/s, it is larger than 1000K. The acoustic temperature measurement technique produces a temperature between T_D and T_A, as expected. Somewhat unexpected is the large effect of the isentropic correction of the temperature by eq. (4). In the present examples the temperature computed with eq. (4) is much closer to T_A than to T_D. The intent of the measurement is to obtain a value for T_D (or T_M). Obviously, the simpler eq. (3) is preferable to eq. (4) for this purpose. The reason for the failure of eq. (4) to improve the temperature is that it is based on assumptions about flow properties which are not met by the computed flow, i.e., by the solution of the one-dimensional flow equations.

Figure 10 shows that the acoustic measurement technique based on eq. (3) is applicable to flows with muzzle velocity of about 500 m/s or less. At 500 m/s the systematic difference between T_D and the measured temperature approaches the magnitude of the observational errors. An extension of the method to cases with higher muzzle velocities requires a better definition of the rarefaction wave front. If eq. (3) is used, then one makes the implicit assumption that the wave front is a straight line in the x,t-plane. The inverse slope of that line is used in eq. (3) as an approximation of the rarefaction wave velocity. An inspection of Figures 8 and 9 suggests that the wave front can be better approximated by a third degree polynomial in t. However, in order to determine such a curve one needs more than the three nodes corresponding to the three pressure gages of the experiment. Therefore, we assume that the device consists of an array of six gages, located at 12.5mm intervals. (Such a device has been also tested at BRL.) Then the task is to fit a third degree polynomial to six nodes or to seven nodes if the muzzle time is included as a seventh observation.

Let x_j be the distances of the six pressure gages from the muzzle and t_j be the corresponding arrival times of the rarefaction wave. Then the constraints for the curve fitting problem are

$$x_j + U_M(t_i - t_M) + U_2(t_i - t_M)^2 + U_3(t_i - t_M)^3 = 0, \qquad (9)$$

$$i = 1, 2, \ldots, 6.$$

The problem has four parameters, namely U_M, t_M, U_2 and U_3. If the muzzle time is used as a seventh observation then the constraint for it is simply

$$t_7 - t_M = 0. \tag{10}$$

After the adjustment the rarefaction wave front $x_r(t)$ and its velocity $u_r(t)$ can be computed by

$$x_r(t) = x_M + U_M(t-t_M) + U_2(t-t_M)^2 + U_3(t-t_M)^3 \tag{11}$$

and

$$u_r(t) = U_M + 2U_2(t-t_M) + 3U_3(t-t_M)^2. \tag{12}$$

At the muzzle the wave has the velocity

$$u_r(t_M) = U_M, \tag{13}$$

and the corresponding temperature is

$$T_M = (u_M - U_M)^2 T_{flame}/(gf). \tag{14}$$

One can also compute the temperature along the rarefaction wave by

$$T_r(t) = (u(t)_{particle} - u_r(t))^2 T_{flame}/(gf), \tag{15}$$

provided that the particle velocity $u_{particle}$ is known. That velocity is generally not constant in the muzzle region, as Figure 11 shows. Only in cases with low muzzle velocities the particle velocity can be approximated by the muzzle velocity u_M. These are the same cases where the temperature is approximately constant within the muzzle region. Therefore, eq. (15) is useless for practical applications and we restrict ourselves to the computation of the muzzle temperature T_M by eq. (14).

The data fittings were carried out using the theoretical data and assuming the same estimates of observational errors as in Section 3, namely

$$\left.\begin{aligned} c_t &= 0.01 \text{ ms}, \\ c_x &= 0.1 \text{ mm}, \\ c_{uM} &= 0.01 \cdot u_M. \end{aligned}\right\} \tag{16}$$

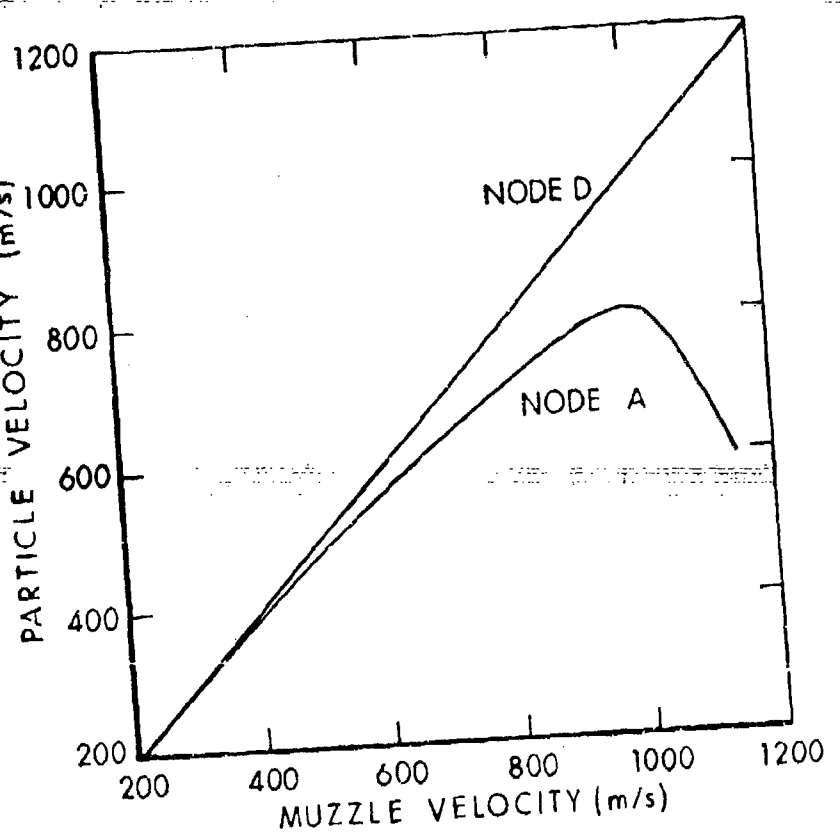

Figure 11. Particle Velocities at Nodes A and D.

Each fitting produced a value of U_M which then was used in eq. (14) to compute T_M. The results are shown in Figure 10. The approximation is excellent up to muzzle velocities of 900 m/s, i.e., up to the limit where rarefaction wave arrivals can be practically observed.

In spite of the good results in the theoretical test, a third degree approximation of the wave front should be used judiciously, because of the sensitivity of the results to observational errors. The standard errors of the fitting parameter U_M and of T_M can be computed using variance propagation formulas and assuming data standard errors as given by eq. (16). The results are shown in Figure 12. They suggest that for low muzzle velocities a third degree approximation induces an unacceptably large uncertainty of the temperature. The reason for the large values of estimated standard errors is the small curvature of the rarefaction wave front. By fitting a high order polynomial to straight line data one introduces redundant parameters, but parameters of redundant sets are strongly correlated and typically have large individual error estimates. The error estimates of T_M from a linear fit (which does not have redundant parameters) are much smaller and of the same order as derived in Section 3. Therefore, one should restrict third order fittings of the rarefaction wave front to cases where the front is clearly not a straight line.

The inclusion of the muzzle time as a seventh observation in the adjustment problem does not change the temperature significantly. The seventh observation does, however, reduce the estimates of the standard errors.

6. CONCLUSIONS.

The acoustic temperature measurement apparatus measures an average temperature for the first few milliseconds in the muzzle flow. The standard error of the measured temperature is about 15%.

One has the following guidelines for the comparison of experimentally measured temperatures with theoretical calculations of the same events:

- Disagreement within 15% is tolerable.
- Temperature peaks of less than one millisecond duration, if existent, cannot be detected by the apparatus, because of its averaging property.
- Disagreements exceeding 15% in a flow without short duration temperature peaks indicate inadequate modeling of the flow.

If the acoustically measured temperature is used to characterize the flow, or is compared with temperature measurements by other techniques,

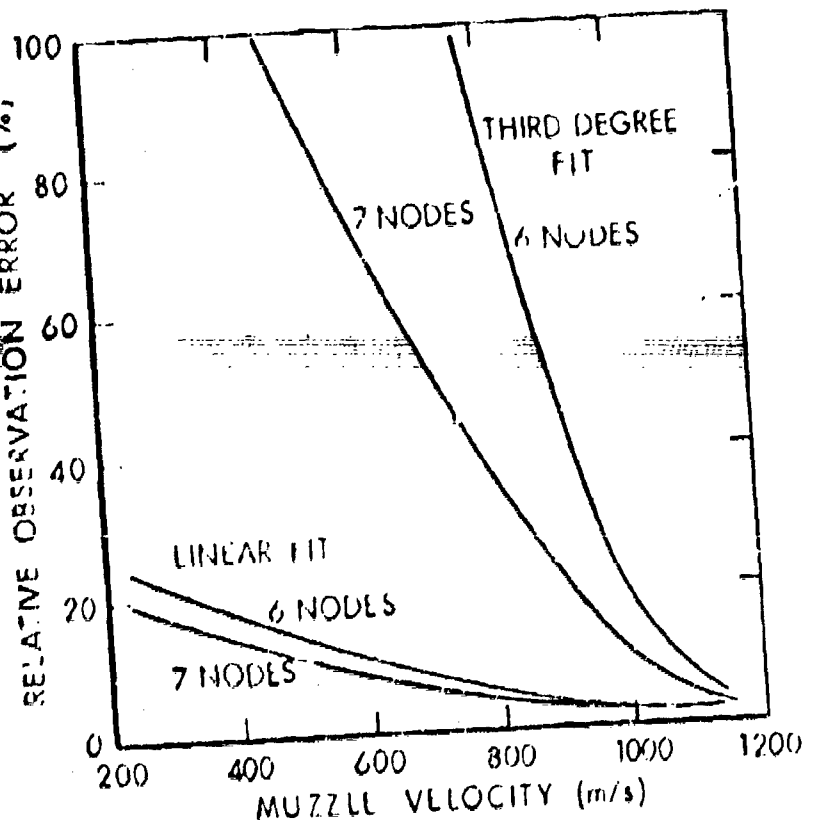

Figure 12. Accuracy of Muzzle Temperature Obtained by Curve Fitting of the Parefaction Wave.

then one should keep in mind the possibility of a systematic error due to an approximate equation of state.

The standard error of the measured temperature can be reduced significantly by increasing the accuracies of the readings of the rarefaction wave's arrival times. A limited reduction of standard observational errors of the temperature could be achieved by making measurements of repeated identical firings.

A reduction of the averaging effect of the technique is possible by increasing the number of pressure gages and using a higher order approximation for the rarefaction wave front. This approach should be used judiciously because it increases the sensitivity of the temperature to observational errors.

REFERENCES

1. E. M. Schmidt, E. J. Gion and D. D. Shear, "Acoustic Thermometric Measurements of Propellant Gas Temperatures in Guns", BRL Report 1919, August 1976. (AD #A030359)

2. A. K. R. Celmiņš, "Theoretical Basis of the Recoilless Rifle Interior Ballistics Code RECRIF", BRL Report 1931, September 1976. (AD #B013832L)

3. A. K. R. Celmiņš, "RECRIF Users' Manual", BRL Memorandum Report 2692, October 1976.

4. W. E. Demming, Statistical Adjustment of Data, J. Wiley & Sons, New York, NY, 1944.

5. S. Shelton, A. Bergler and P. Saha, "Study of Heat Transfer and Erosion Rate in Gun Barrels", Air Force Armament Laboratory Technical Report TR-73-69, March 1973.

6. R. Heiser, "Hodographenverfahren für Instationäre Eindimensionale Gasströmungen", PhD Thesis, Technical University Aachen, FRG, December 1975.

DISTRIBUTION LIST

No. of Copies	Organization
4	Commander US Army Armament Research and Development Command ATTN: DRDAR-SC/Mr. S. Hirschman Mr. F. Puzycki DRDAR-SCN/Mr. Kahn DRDAR-SCW/Mr. Townsend Dover, NJ 07801
4	Commander US Army Armament Research and Development Command ATTN: DRDAR-LC-F/Mr. A. Loeb Mr. E. Friedman DRDAR-LCV/Mr. Barrieres Mr. R. Reisman Dover, NJ 07801
2	Product Manager 30mm Ammunition ATTN: LTC Delaney Mr. A. Ciancosi US Army Armament Research and Development Command Dover, NJ 07801
4	Chief Benet Weapons Laboratory US Army Armament Research and Development Command ATTN: DRDAR-LCB-TL SARWV-PDR-S/F. Sautter SARWV-PDR-AMM Dr. J. Zweig SARWV-RDD-SE/P.A. Alto Watervliet, NY 12189
1	Commander US Army Armament Materiel Readiness Command ATTN: DRSAR-LEP-L/Tech Lib Rock Island, IL 61299
1	Commander US Army Jefferson Proving Ground ATTN: STEJP-TD-D Madison, IN 47250
1	Commander US Army Materials and Mechanics Research Center ATTN: DRXMR-ATL Watertown, MA 02172
1	Commander US Army Natick Research and Development Command ATTN: DRXRE/Dr. D. Sieling Natick, MA 01762
1	Director US Army TRADOC Systems Analysis Activity ATTN: ATAA-SL/Tech Lib White Sands Missile Range, NM 88002
1	HQDA (DAMA-WSA, MAJ Fite) Washington, DC 20310
1	Commander US Army Research Office ATTN: CRD-AA-EH P. O. Box 12211 Research Triangle Park, NC 27709
1	Director US Army BMD Advanced Technology Center P. O. Box 1500, West Station Huntsville, AL 35807
1	Commander US Army Ballistic Missile Defense Systems Command Huntsville, AL 35804

DISTRIBUTION LIST

No. of Copies	Organization
1	Commander US Army Advanced Materiel Concepts Agency 5001 Eisenhower Avenue Alexandria, VA 22333
3	Commander US Naval Air Systems Command ATTN: AIR-604 Washington, DC 20360
3	Commander US Naval Ordnance Systems Command ATTN: ORD-9132 Washington, DC 20360
2	Commander and Director David W. Taylor Naval Ship Research & Development Ctr ATTN: Tech Lib Aerodynamic Lab Bethesda, MD 20084
3	Commander US Naval Surface Weapons Ctr ATTN: Code 312/Mr. F. Regan Mr. S. Hastings Code 730/Tech Lib Silver Spring, MD 20910
3	Commander US Naval Surface Weapons Ctr ATTN: Code GX/Dr. Yagla Mr. F. H. Maille Dr. G. Moore Dahlgren, VA 22448
1	Commander US Naval Weapons Center ATTN: Code 553/Tech Lib China Lake, CA 93555
3	Commander US Naval Research Laboratory ATTN: Tech Info Div Code 7700/D. A. Kolb Code 7720/Dr. E. McClean Washington, DC 20375
1	Commander US Naval Ordnance Station ATTN: Code FS13A/P. Sewell Indian Head, MD 20640
1	AFRPL/LKCB (Dr. Horning) Edwards AFB, CA 93523
1	ADTC (ADBPS-12) Eglin AFB, FL 32542
1	AFATL (DLDL) Eglin AFB, FL 32542
1	AFATL (Tech Lib) Eglin AFB, FL 32542
1	AFWL (DEV) Kirtland AFB, NM 87117
1	ASD/XRA (Stinfo) Wright-Patterson AFB, OH 45433
1	Director NASA Scientific and Technical Information Facility ATTN: SAK/DL P. O. Box 8757 Baltimore/Washington International Airport, MD 21240
1	Director Jet Propulsion Laboratory ATTN: Tech Lib 2800 Oak Grove Drive Pasadena, CA 91103

DISTRIBUTION LIST

No. of Copies	Organization
1	Director National Aeronautics and Space Administration George C. Marshall Space Flight Center ATTN: MS-I/Lib R-AERO-AE/A Felix Huntsville, AL 35812
1	Director National Aeronautics and Space Administration Langley Research Center ATTN: MS 185/Tech Lib Langley Station Hampton, VA 23365
1	AAI Corporation ATTN: Dr. T. Stastny Cockeysville, MD 21030
1	Advanced Technology Labs ATTN: Dr. J. Erdos Merrick & Stewart Avenues Westbury, NY 11590
1	Aerospace Corporation ATTN: Dr. T. Taylor P. O. Box 92957 Los Angeles, CA 90009
2	ARO, Inc. ATTN: Tech Lib Dr. J. Adams Arnold AFS, TN 37389
1	ARTEC Associates, Inc. ATTN: Dr. S. Gill 26046 Eden Landing Road Hayward, CA 94545
1	AVCO Systems Division ATTN: Dr. W. Reinecke 201 Lowell Street Wilmington, MA 01887
1	Battelle Columbus Laboratories ATTN: J. E. Backofen, Jr. 505 King Avenue Columbus, OH 43201
1	Calspan Corporation ATTN: Mr. G. A. Sterbutzel P. O. Box 235 Buffalo, NY 14221
1	Technical Director Colt Firearms Corporation 150 Huyshore Avenue Hartford, CT 14061
1	General Electric Corporation Armaments Division ATTN: Mr. R. Whyte Lakeside Avenue Burlington, VT 05401
1	Martin Marietta Aerospace ATTN: Mr. A. J. Culotta P. O. Box 5387 Orlando, FL 32805
1	Winchester-Western Division Olin Corporation New Haven, CT 06504
1	Rockwell Int'l Science Center ATTN: Dr. Norman Malmuth P. O. Box 1085 1000 Oaks, CA 91360
1	Sandia Laboratories ATTN: Aerodynamics Department Org 5620, R. Maydew Albuquerque, NM 87115

DISTRIBUTION LIST

No. of Copies	Organization
1	S&D Dynamics, Inc. ATTN: Dr. M. Soifer 755 Ndw York Avenue Huntington, NY 11743
1	Guggenheim Aeronautical Laboratory California Institute of Technology ATTN: Tech Lib Pasadena, CA 91104
1	Franklin Institute ATTN: Dr. Carfagno Dr. Wachtell Race & 20th Streets Philadelphia, PA 19103
1	Director Applied Physics Laboratory The Johns Hopkins University Johns Hopkins Road Laurel, MD 20810
1	Massachusetts Institute of Technology Department of Aeronautics and Astronautics ATTN: Tech Lib 77 Massachusetts Avenue Cambridge, MA 02139
1	Ohio State University Department of Aeronautics and Astronautical Engineering ATTN: Tech Lib Columbus, OH 43210
2	Polytechnic Institute of Brooklyn Graduate Center ATTN: Tech Lib Dr. G. Moretti Farmingdale, NY 11735
1	Forrestal Campus Library Princeton University ATTN: Dr. M. Summerfield P. O. Box 710 Princeton, NJ 08540
1	Southwest Research Institute ATTN: Mr. Peter S. Westine P. O. Drawer 28510 8500 Culebra Road San Antonio, TX 78228

Aberdeen Proving Ground

Dir, USAMSAA
ATTN: Dr. J. Sperrazza
DRXSY-MP, H. Cohen
Cdr, USA CSL/EA
ATTN: A. Flatau, SAREA-DE-W
Bldg. E-3516